

## A kinetic model of the formation of the hot oxygen geocorona

### 2. Influence of O<sup>+</sup> ion precipitation

D. V. Bisikalo and V. I. Shematovich

Institute of Astronomy, Russian Academy of Sciences, Moscow

J.-C. Gérard

Laboratoire de Physique Atmosphérique et Planétaire, Institut d'Astrophysique, Université de Liège, Liège  
Belgium

**Abstract.** A model of the oxygen geocorona near the exobase solving the nonlinear Boltzmann equation with a Monte Carlo method is used to calculate the distribution of the hot oxygen atoms during geomagnetically disturbed nighttime conditions. The precipitation of energetic O<sup>+</sup> ions and the subsequent enhancement of the hot O corona at high latitudes is simulated for the September 17, 1971, storm conditions. It is found that in such circumstances, the O<sup>+</sup> precipitation is a significant source of superthermal O atoms leading to important perturbations of the velocity distribution of the bulk oxygen population. The effective gas temperature near the exobase is similar to that in the undisturbed atmosphere, but the hot O density rises considerably over the quiet condition values.

### 1. Introduction

The possible existence of nonthermal atomic oxygen in the high-altitude region of the Earth's atmosphere has been considered theoretically and experimentally by various workers over the years [Hays and Walker, 1966; Hernandez, 1971; Rohrbaugh and Nisbet, 1973; Torr et al., 1974; Yee and Hays, 1980; Yee et al., 1980; Kozyra et al., 1982; Ishimoto et al., 1986, 1992; Yee and Killeen, 1986; Hedin, 1989]. Chemical energy of photodissociation of O<sub>2</sub>, dissociative recombination of O<sub>2</sub><sup>+</sup> and NO<sup>+</sup> ions, quenching of N(<sup>2</sup>D), O(<sup>1</sup>D), O(<sup>1</sup>S) and other chemical sources [Richards et al., 1994] and precipitated O<sup>+</sup> energy during magnetic storms are the major sources of nonthermal atoms. There is also experimental evidence of the existence of a hot oxygen geocorona [Hernandez, 1971; Yee et al., 1980; Hedin, 1989; Cotton et al., 1993]. The long-term presence of nonthermal oxygen atoms would have considerable influence on the properties of the upper atmosphere [e.g., Hedin, 1989].

In our previous work [Shematovich et al., 1994] (hereinafter referred to as paper 1), we numerically studied the hot O geocorona formation due to chemical sources (O<sub>2</sub> photodissociation and O<sub>2</sub><sup>+</sup> and NO<sup>+</sup> dissociative recombination). It was shown that during daytime and in quiet geomagnetic conditions there is a significant amount of fast O atoms above 300 km and that hot oxygen could be an important component of the exosphere.

It is known that the precipitating fluxes of energetic O<sup>+</sup> ions observed during magnetic storms are a major source of energy into the upper atmosphere [Torr et al., 1974; Kozyra et al., 1982; Ishimoto et al., 1992]. Energetic O<sup>+</sup> ions also may be considered as an additional source of fast oxygen atoms.

In this paper we present a numerical kinetic model of the

hot O geocorona formation due to O<sup>+</sup> ion precipitation in the nighttime upper atmosphere and for disturbed geomagnetic conditions. To investigate this problem, we use the stochastic simulation method described in details in paper 1. The main feature of this numerical kinetic approach is the possibility to consider the nonlinear collisional interactions between the thermal and nonthermal populations of the atmospheric gas.

Attempts were made previously to investigate the behavior of nonthermal particles in the transition region of the atmosphere. Previously, linearized Boltzmann equations were used for the description of the gas flow in this region (Monte Carlo probe particle method [Hodges and Breig, 1993], multistream and two-stream methods [Torr et al., 1974; Kozyra et al., 1982; Ishimoto et al., 1992], and solution of Liouville's theorem [Yee and Hays, 1980]). These numerical methods allow the evaluation of several effects induced by O<sup>+</sup> precipitation (escape fluxes, heating rate of the atmospheric gas, optical emission rates, etc.). However, as was discussed in paper 1, the formation of the hot O geocorona is essentially a nonlinear problem because it is formed mostly by the disturbed thermal fraction of the ambient atmospheric gas. Consequently, it may be described completely only by a set of nonlinear kinetic Boltzmann equations.

The stochastic method (described in paper 1) adopted here allows solution of the system of nonlinear kinetic equations and is used in this work to investigate the role of O<sup>+</sup> ion precipitation in hot oxygen corona formation. We show that the precipitation of O<sup>+</sup> energetic ions substantially modifies the velocity distribution function of the ambient O atoms, raises the effective kinetic temperature, and increases the density of hot atoms over the quiet daytime values.

### 2. Model

#### 2.1. The Physical Model

In this work we study the hot oxygen geocorona formation due to the precipitation of O<sup>+</sup> ions in the transition region of

the Earth's atmosphere (i.e., at heights of 200–800 km). At the lower boundary of this region, the number density of the atmospheric gas is sufficiently high (Knudsen number  $Kn \leq 0.1$ ) to consider the thermal state of the gas to be close to local thermodynamic equilibrium (LTE). At the upper boundary of the transition region the Knudsen number for gas flow  $Kn \sim 1$ , and consequently, a collisionless regime of atmospheric gas flow is assumed.

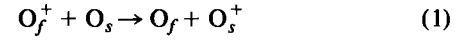
For the main purpose of this study (the investigation of hot geocorona formation) the lower boundary should be defined in the region where the upward fluxes of nonthermal particles are vanishing. For the atmospheric conditions considered in this study, this region is about 300 km (paper 1). Above 300 km, O is the dominant component of the atmospheric gas, and therefore in this model we consider only interactions with one component, atomic oxygen. In this study we also investigate another effect of the ion flux precipitation: the heating of the neutral gas. This effect was intensively studied [Torr *et al.*, 1974; Kozyra *et al.*, 1982; Ishimoto *et al.*, 1986, 1992], and consequently, its numerical calculation may be considered as a test of our model. From previous studies it is known that the peak of the heating rate lies in the region 200–300 km, and therefore we adopt 200 km as the lower boundary. The heating rate of the atmospheric gas is determined by elastic collisions of nonthermal particles with the ambient gas, which consists of an N<sub>2</sub> and O mixture at altitudes of less than 300 km. For a gas in local equilibrium it is possible to account for the gas composition by modifying the collision frequency in the one-component model [Bird, 1976]. This approach is used for the sake of simplicity, and only one component, atomic oxygen, is considered. In the region where the densities of O and N<sub>2</sub> become comparable (below 300 km), we take into account the N<sub>2</sub> input into the relaxation properties of the gas by increasing the elastic collision frequency by the appropriate amount.

The first observation of precipitation of energetic heavy ions into the atmosphere was reported by Shelley *et al.* [1972]. Further observational information on the energetic O<sup>+</sup> ions were described in a series of papers [Shelley *et al.*, 1974; Sharp *et al.*, 1974, 1976a, b]. The measurements were made at an altitude of 800 km over an energy range of 0.7–12 keV. The fluxes of O<sup>+</sup> precipitation were found to occur over a wide latitudinal range, covering  $L$  shells  $2 < L < 9$ , and were observed in every storm studied over a 1-year period. They were also found to occur at reduced intensities during nonstorm conditions. Most of the observations were made at a pitch angle of 55°–58°. These measurements were significant because the fluxes of fast O<sup>+</sup> were found to be relatively large during the magnetic storm events. These events carry energy fluxes as large as  $0.4 \text{ erg cm}^{-2} \text{ s}^{-1} \text{ sr}^{-1}$  at 800 km over extended time periods. Energy fluxes of about  $0.1 \text{ erg cm}^{-2} \text{ s}^{-1} \text{ sr}^{-1}$  were frequently observed. The energetic oxygen ions have been observed at all local times, but the dayside fluxes were typically found to be 5–10 times less than those measured on the nightside [Sharp *et al.*, 1976a].

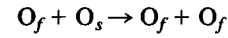
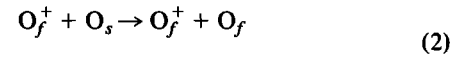
In this study, we use the O<sup>+</sup> energy spectrum measured by Shelley *et al.* [1972] during the December 17, 1971, storm corresponding to  $L \sim 3.4$  (i.e., at a latitude of 45°). The incident O<sup>+</sup> flux was injected isotropically into the downward hemisphere, carrying an energy flux of about  $0.4 \text{ erg cm}^{-2} \text{ s}^{-1}$  (as adopted by Torr *et al.* [1982]). We use the mass

spectrometer–incoherent scatter (MSIS) 90 model [Hedin, 1991] for solar maximum ( $F_{10.7} = 200$ ) at a local time of 0300 for magnetically disturbed conditions ( $Ap = 100$ ) in the northern hemisphere in December. In this model we consider only one component of the atmosphere gas: atomic oxygen, by far the dominant component of the atmospheric gas at the altitude of the transition region.

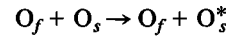
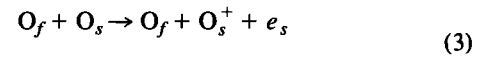
Precipitating energetic O<sup>+</sup> ions interact with ambient gas in the following processes: (1) conversion of energetic O<sup>+</sup> ions to fast neutral atoms by resonance charge transfer



where the subscripts  $f$  and  $s$  refer to fast and slow atoms, respectively; (2) momentum transfer processes in which fast ions and atoms collide elastically with the ambient O atoms



and share kinetic energy; and (3) excitation of the ambient gas by the small fraction of the fast atoms with sufficient energy to ionize



The relative importance of processes (1)–(3) is governed by their collision cross sections. At primary energies below about 10 keV, virtually all the energy goes into channels (1) and (2) [Rees, 1989]. In our calculations we use the measured [Shelley *et al.*, 1972] O<sup>+</sup> flux with energies up to 12 keV, and therefore in the model we consider only reactions (1) and (2) and do not include (3).

The charge exchange cross sections ( $\sigma_{ch}$ ) for collisions of energetic O<sup>+</sup> on O measured by Rutherford and Vroom [1974] and Stebbings *et al.* [1964] are adopted. The total cross sections ( $\sigma_{el}$ ) used for elastic collisions of energetic O<sub>f</sub><sup>+</sup> and O<sub>f</sub> on O are energy dependent and of the order of  $1.7 \times 10^{-15} \text{ cm}^2$  at 1 keV [Kozyra *et al.*, 1982; Rees, 1989]. The dominant feature of the elastic collisions of fast O<sub>f</sub> atoms on O is that the elastic differential scattering cross sections (DSCS) for this interaction are strongly forward peaked [Kozyra *et al.*, 1982]. Unfortunately, we could not find measured DSCS for elastic O–O collisions. Therefore we used the measured DSCS for elastic collisions of energetic O on O<sub>2</sub> [Schafer *et al.*, 1987], processed in the manner described by Ishimoto *et al.* [1992].

## 2.2. The Mathematical Model

The physical system taking into account the production, elastic and inelastic relaxation, and transport processes for the O atoms and ions in the transition region may be strictly described by a system of Boltzmann type kinetic equations (paper 1):

$$\begin{aligned} \frac{\partial}{\partial t} F_f + \mathbf{c} \frac{\partial}{\partial \mathbf{r}} F_f + \mathbf{S} \frac{\partial}{\partial \mathbf{c}} F_f = J_{ch}(F_f; F_{th}, F_i) \\ + J_{el}(F_f, F_{th}) + J_{el}(F_f, F_i) \end{aligned}$$

$$\begin{aligned}
\frac{\partial}{\partial t} F_i + \mathbf{c} \frac{\partial}{\partial \mathbf{r}} F_i + \mathbf{S} \frac{\partial}{\partial \mathbf{c}} F_i &= J_{\text{ch}}(F_i; F_{\text{th}}, F_f) \\
&+ J_{\text{el}}(F_i, F_{\text{th}}) + J_{\text{el}}(F_i, F_f) \\
\frac{\partial}{\partial t} F_{\text{th}} + \mathbf{c} \frac{\partial}{\partial \mathbf{r}} F_{\text{th}} + \mathbf{S} \frac{\partial}{\partial \mathbf{c}} F_{\text{th}} &= J_{\text{ch}}(F_{\text{th}}; F_f, F_i) \\
&+ \sum_{L=\text{th}, f, i} J_{\text{el}}(F_{\text{th}}, F_L)
\end{aligned} \tag{4}$$

where  $\mathbf{r}$  and  $\mathbf{c}$  are the space coordinate and velocity of gas particles,  $F_{\text{th}}$  is the distribution function for thermal atoms of the ambient gas, and  $F_f$  and  $F_i$  are the distribution functions for superthermal  $\text{O}_f$  atoms and for  $\text{O}^+$  ions.

The particle transport in the gravitational Earth's force field  $\mathbf{S}$  is described by the left-hand side of (4), whereas the right-hand side describes the collisional evolution of the atmospheric gas. The share of kinetic energy of fast  $\text{O}_f$  atoms and  $\text{O}_f^+$  ions in elastic collisions with the ambient gas is described by the collision integrals

$$\begin{aligned}
J_{\text{el}}(F_f, F_{\text{th}}) &= \int |\mathbf{c}_f - \mathbf{c}_{\text{th}}| [F_f(\mathbf{c}'_f) F_{\text{th}}(\mathbf{c}'_{\text{th}}) \\
&- F_{\text{th}}(\mathbf{c}_{\text{th}}) F_f(\mathbf{c}_f)] \sigma_{\text{el}} d\mathbf{c}_{\text{th}},
\end{aligned}$$

where  $\mathbf{c}'$  is the particle velocity after collision. These integrals include all possible channels of elastic collisional interactions: the cascade formation of secondary nonthermal  $\text{O}_f$  atoms, the disturbances of thermal atoms, the thermalization of nonthermal and thermal fractions, etc. In the right-hand side of system (4) also appears the charge exchange collision integral

$$J_{\text{ch}} = \int |\mathbf{c}_i - \mathbf{c}_{\text{th}}| [F_f F_i - F_{\text{th}} F_i] \sigma_{\text{ch}} d\mathbf{c}_i$$

which describes the source of superthermal atoms and of ions and thermal atoms.

A qualitative analysis (the same as in paper 1) of these integrals shows that in the transition region considered, significant perturbations of the thermal state are possible. This means that the kinetic system considered becomes nonlinear and, consequently, that a stochastic simulation method must be used to solve this system.

### 2.3. Numerical Aspects

The main properties of the numerical method used here were presented in paper 1. In the numerical experiment the evolution of the system of modeling particles from the initial state to steady state is calculated. In agreement with the stochastic simulation method, this numerical system of modeling particles approximates the solution of the initial kinetic system (4). In this case it is possible to use the distribution functions statistically estimated in the numerical simulation to calculate all the necessary gas macroscopic properties describing the atmospheric gas flow in the transition region of the Earth's atmosphere.

The following modifications of the scheme were introduced for the present calculations: (1) The transition region from the thermosphere to the exosphere (200–800 km) under study was divided into a system of 24 radial cells. The

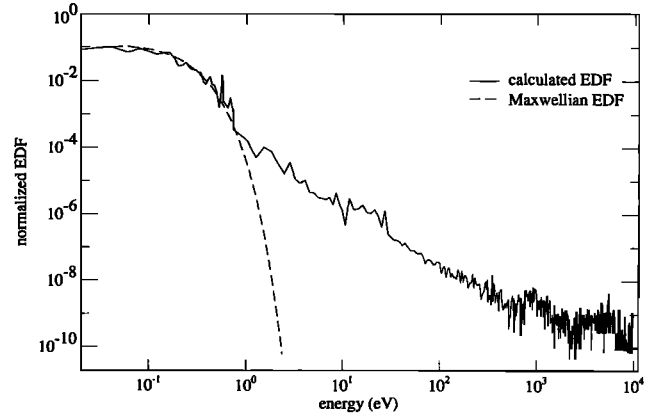


**Figure 1.** Energy distribution functions (EDF) for atomic oxygen in the transition region at 500 km. The solid line shows the calculated distribution and the dashed line represents the local Maxwellian distribution function ( $T = 1170$  K).

altitude dependent cell size was chosen from the condition that it must be equal to or smaller than the free path length near the lower boundary of each cell. (2) We include an additional component in the model particle gas to describe the  $\text{O}^+$  ions. This component is defined in the numerical system by a steady state inflow of modeling particles at the upper boundary (800 km) distributed according to a given energy spectrum. All other components (thermal and nonthermal O atoms) were modeled in the same manner as in paper 1.

### 3. Results

In the numerical experiments we have carried out, the steady state kinetic energy distribution functions for atomic oxygen were calculated. An example of the calculated distribution function at altitude 500 km is given in Figure 1. This function is normalized to 1 by the oxygen density. The dashed curve on the figure corresponds to a Maxwellian distribution function for the local temperature ( $T = 1170$  K). It is seen that the steady state kinetic energy distribution function is strongly out of equilibrium and departs significantly from the local Maxwellian distribution, especially at high energies. In our calculations, it was found that these nonthermal perturbations increase with the height because the relaxation properties of the atmospheric gas decrease with the altitude in the transition region.

The analysis of the energy distribution functions suggests to formally divide the atomic oxygen atoms into three components: (1) a thermal component, i.e., the atoms whose kinetic energy distribution may be described as Maxwellian; (2) a superthermal fraction, including fast O atoms produced in charge exchange and momentum transfer processes with energies greater than the escape energy; and (3) an overthermal fraction, i.e., atoms produced by the thermalization of the superthermal fraction to energies less than the escape energy ( $\sim 10.4$  eV) and due to perturbations of the thermal fraction in their interaction with overthermal and superthermal atoms. This formal distinction is useful for the analysis of the numerical results, since the macroscopic characteristics of the  $\text{O}^+$  precipitation (escape flux, heating rate, etc.)

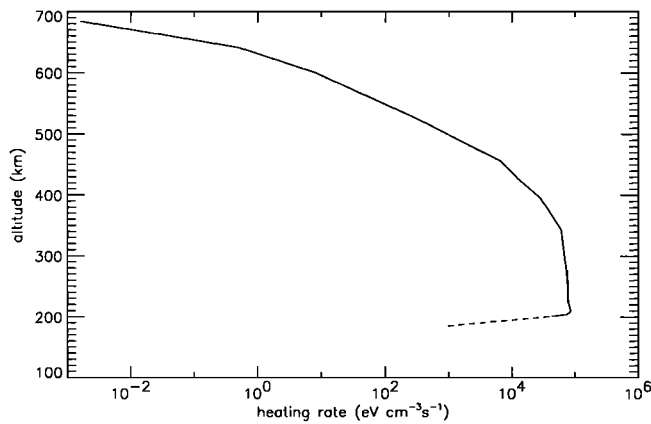


**Figure 2.** Vertical distribution of the atmospheric heating rate due to  $O^+$  precipitation during a geomagnetically disturbed period (see text). The rate of energy transfer to the ambient gas is calculated from the nonequilibrium energy distribution function of the  $O^+$  ions and  $O$  atoms.

are defined by the superthermal fraction, whereas the hot oxygen corona formation is dominated by the overthermal fraction (paper 1).

The calculated energy distribution functions provide all the macroscopic quantities describing the  $O^+$  ion precipitation. For example, we evaluate the energy escape flux at about 12%, a value in agreement with previous studies [Kozyra *et al.*, 1982; Ishimoto *et al.*, 1986, 1992]. Another significant macroscopic quantity linked to the  $O^+$  ion precipitation is the heating rate of the neutral gas. The vertical distribution of the heating rate is characterized by a peak of  $8.6 \times 10^4 \text{ eV cm}^{-3} \text{ s}^{-1}$  near 200 km and a very slow decrease up to 340 km (Figure 2). These values are in good agreement with previous investigations using two-stream or multistream methods.

In addition to the energy deposition and other macroscopic properties of the  $O^+$  precipitation, the calculated energy distribution functions provide information useful for investigating the hot  $O$  geocorona.

The formation of the hot  $O$  geocorona due to the  $O^+$  ion precipitation may be analyzed in detail by using the calculated energy distribution functions of atomic oxygen in the transition region. It is found that the hot  $O$  geocorona is formed mostly by the overthermal gas fraction consisting of the disturbed thermal atoms and the partly thermalized superthermal atoms. The superthermal fraction has a much lower density, but nevertheless, these energetic particles have a significant influence on the oxygen geocorona temperature.

Examples of kinetic energy distribution functions of steady state for thermal and overthermal fractions of atomic oxygen are given in Figure 3. In this plot, the distribution functions normalized to 1 by the oxygen density are presented at of 400, 500, and 600 km. The local Maxwellian distribution function is also shown for comparison.

From these functions it is possible to define the main macroscopic parameters of the hot  $O$  geocorona: the temperature and density vertical profiles. We define the temperature and density of hot oxygen based on a criterium dividing between the thermal and nonthermal fractions. As in paper 1, we set the limit where the steady state energy distribution

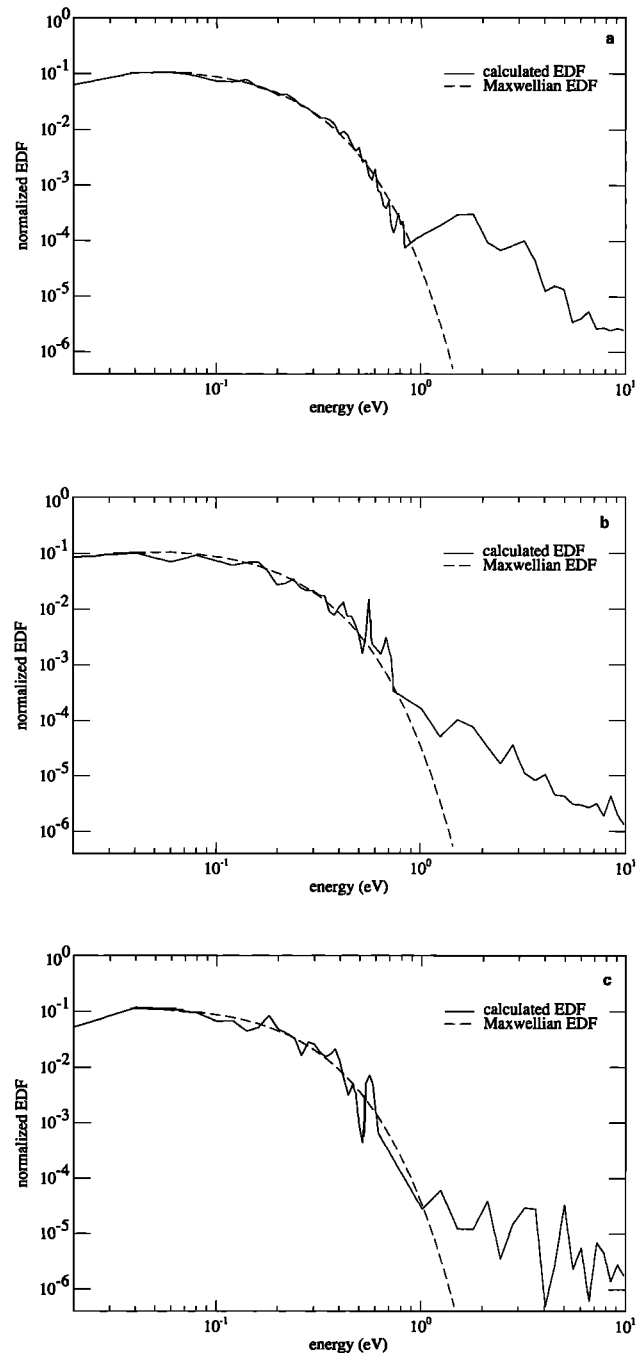


**Figure 3.** Energy distribution functions (EDF) for the thermal and overthermal populations of atomic oxygen in the transition region: (a) 400 km, (b) 500 km, and (c) 600 km. The solid line shows the calculated distribution, and the dashed line represents the local Maxwellian distribution function.

function differs from the Maxwellian one by more than the precision of our calculation (5%). The height profiles of density for hot and thermal fractions of  $O$  atoms are given in Figure 4. The density of the hot  $O$  atoms varies from  $1.0 \times 10^7 \text{ cm}^{-3}$  at 300 km to  $9.0 \times 10^5 \text{ cm}^{-3}$  at 790 km. The temperature of the hot  $O$  is about 4100 K for all altitudes. Figure 4 shows that the density scale height for hot  $O$  is larger than the one for the thermal fraction. It is also seen

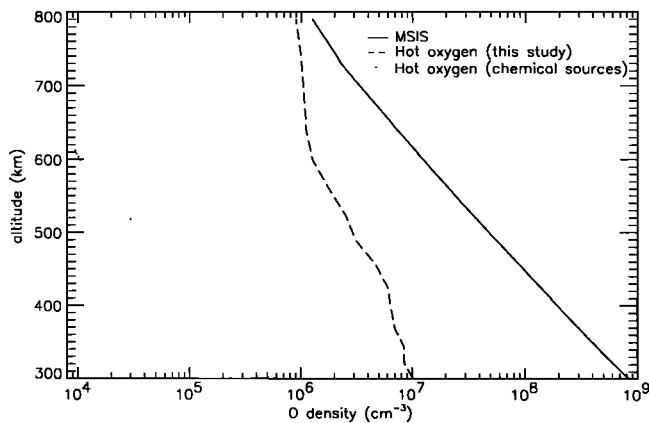


**Figure 4.** Vertical profiles of the hot and thermal fractions of atomic oxygen in the transition region. The dashed line is the hot fraction and the solid line is the MSIS density profile of thermal oxygen. For comparison, the hot O density produced by chemical sources (paper 1) (dotted line) is also presented.

that at heights above  $\sim 800$  km the density of hot O becomes dominant in the exosphere.

The results of the calculations presented here show that the precipitation of  $O^+$  ion during geomagnetic storms is a significant source of superthermal O atoms. The comparison with the results of paper 1 (see Figure 4) shows that the hot O geocorona due to the  $O^+$  ion precipitation is significantly more abundant than that due to chemical sources but that the corona temperature is practically unchanged. It should be noted that this comparison has an illustrative nature, since the results presented in this study and in paper 1 are obtained under different geophysical conditions.

These calculations are also in agreement with the estimates of the hot O density for high solar activity derived from differences between satellite drag and mass spectrometer based models [Hedin, 1989]. At altitudes of about 550 km, our calculated density is about  $1.7 \times 10^6 \text{ cm}^{-3}$  compared with Hedin's values of  $5 \times 10^5$  to  $2 \times 10^6 \text{ cm}^{-3}$ . At 925 km the measured values are  $1\text{--}4 \times 10^5 \text{ cm}^{-3}$ , and extrapolation of our results gives a value of about  $4\text{--}5 \times 10^5 \text{ cm}^{-3}$ .

#### 4. Conclusions

In this work an adaptation of the model of the hot O geocorona formation in the transition region to the case of precipitation of energetic ions is presented. This model, in analogy to paper 1, includes a full solution of the nonlinear collisional interaction between thermal ambient gas and superthermal particles. These superthermal particles are produced by the  $O^+$  ion precipitation during the magnetic storm.

The analysis of the calculated kinetic energy distribution functions for thermal, overthermal, and superthermal fractions of atomic oxygen yields the following conclusions: (1) The  $O^+$  ion precipitation is a significant source of superthermal O atoms, exceeding by far the chemical sources of the quiet daytime conditions. (2) The nonlinear collisional interaction between the superthermal and thermal fractions of atomic oxygen leads to strong disturbances of the ambient

atmospheric gas, i.e., to the formation of an overthermal gas fraction. These overthermal atoms are the main source of the hot O geocorona. (3) The calculated parameters of the hot O geocorona are in agreement with the available experimental estimates.

**Acknowledgments.** J. C. Gérard is supported by the Belgian Foundation for Scientific Research (FNRS), and V. I. Shematovich and D. V. Bisikalo are supported by the Russian Foundation for Fundamental Research (RFFR) and by the International Science Foundation (ISF). This research was partly financed by grants FRFC 2.4539.93, RFFR 93-02-2847, and ISF MM8000.

#### References

- Bird, G. A., *Molecular Gas Dynamics and the Direct Simulation of Gas Flows*, Clarendon, Oxford, 1994.
- Cotton, D. M., G. R. Gladstone, and S. Chakrabarti, Sounding rocket observation of a hot atomic oxygen geocorona, *J. Geophys. Res.*, **98**, 21,651, 1993.
- Hays, P. B., and J. C. G. Walker, Doppler profiles of 5577 Å airglow, *Planet. Space Sci.*, **14**, 1331, 1966.
- Hedin, A. E., Hot oxygen geocorona as inferred from neutral exospheric models and mass spectrometer measurements, *J. Geophys. Res.*, **94**, 5523, 1989.
- Hedin, A. E., Extension of the MSIS thermosphere model into the middle and lower atmosphere, *J. Geophys. Res.*, **96**, 1159, 1991.
- Hernandez, G., The signature profile of  $O(^1S)$  in the airglow, *Planet. Space Sci.*, **19**, 468, 1971.
- Hodges, R. R., and E. L. Breig, Charge transfer and momentum exchange in exospheric  $D\text{-H}^+$  and  $H\text{-D}^+$  collisions, *J. Geophys. Res.*, **98**, 1581, 1993.
- Ishimoto, M., M. R. Torr, P. G. Richards, and D. G. Torr, The role of energetic  $O^+$  precipitation in a mid-latitude aurora, *J. Geophys. Res.*, **91**, 5793, 1986.
- Ishimoto, M., G. J. Romick, and C.-I. Meng, Energy distribution of energetic  $O^+$  precipitation into the atmosphere, *J. Geophys. Res.*, **97**, 8619, 1992.
- Kozyra, J. V., T. E. Cravens, and A. F. Nagy, Energetic  $O^+$  precipitation, *J. Geophys. Res.*, **87**, 2481, 1982.
- Rees, M. H., *Physics and Chemistry of the Upper Atmosphere*, Cambridge University Press, New York, 1989.
- Richards, P. G., M. P. Hickey, and D. G. Torr, New sources for the hot oxygen geocorona, *Geophys. Res. Lett.*, **21**, 657, 1994.
- Rohrbaugh, R. P., and J. S. Nisbet, Effect of energetic oxygen atoms on neutral density models, *J. Geophys. Res.*, **78**, 6768, 1973.
- Rutherford, J. A., and D. A. Vroom, The reaction of atomic oxygen with several atmospheric ions, *J. Chem. Phys.*, **61**, 2514, 1974.
- Schafer, D. A., J. H. Newman, K. A. Smith, and R. F. Stebbings, Differential cross sections for scattering of 0.5-, 1.5-, and 5.0-keV oxygen atoms by  $He$ ,  $N_2$ , and  $O_2$ , *J. Geophys. Res.*, **92**, 6107, 1987.
- Sharp, R. D., R. E. Johnson, and E. G. Shelley, The morphology of energetic  $O^+$  in the magnetosphere, *J. Geophys. Res.*, **79**, 144, 1974.
- Sharp, R. D., R. E. Johnson, and E. G. Shelley, The morphology of energetic  $O^+$  ions during two magnetic storms: Temporal variations, *J. Geophys. Res.*, **81**, 3283, 1976a.
- Sharp, R. D., R. E. Johnson, and E. G. Shelley, The morphology of energetic  $O^+$  ions during two magnetic storms: Latitudinal variations, *J. Geophys. Res.*, **81**, 3292, 1976b.
- Shelley, E. G., R. E. Johnson, and R. D. Sharp, Satellite observation of energetic heavy ions during a geomagnetic storm, *J. Geophys. Res.*, **77**, 6104, 1972.
- Shelley, E. G., R. E. Johnson, and R. D. Sharp, The morphology of energetic  $O^+$  in the magnetosphere, in *Magnetospheric Physics*, pp. 135-139, D. Reidel, Norwell, Mass., 1974.
- Shematovich, V. I., D. V. Bisikalo, and J.-C. Gérard, A kinetic model of the formation of the hot oxygen geocorona, 1, Quiet geomagnetic conditions, *J. Geophys. Res.*, **99**, 23,217, 1994.
- Stebbins, R. F., A. C. H. Smith, and H. Ehrhardt, Charge transfer between oxygen atoms and  $O^+$  and  $H^+$  ions, *J. Geophys. Res.*, **69**, 2349, 1964.

- Torr, M. R., J. C. G. Walker, and D. G. Torr, Escape of fast oxygen from the atmosphere during geomagnetic storms, *J. Geophys. Res.*, **79**, 5267, 1974.
- Torr, M. R., D. G. Torr, R. G. Roble, and E. C. Ridley, The dynamic response of the thermosphere to the energy influx resulting from energetic  $O^+$  ions, *J. Geophys. Res.*, **87**, 5290, 1982.
- Yee, J. H., and P. B. Hays, The oxygen polar corona, *J. Geophys. Res.*, **85**, 1795, 1980.
- Yee, J. H., and T. L. Killeen, Thermospheric production of  $O(^1S)$  by dissociative recombination of vibrationally excited  $O_2^+$ , *Planet Space Sci.*, **34**, 1101, 1986.
- Yee, J. H., J. W. Meriwether, and P. B. Hays, Detection of a corona of fast oxygen atoms during solar maximum, *J. Geophys. Res.*, **85**, 3396, 1980.
- 
- D. V. Bisikalo and V. I. Shematovich, Institute of Astronomy, Russian Academy of Sciences, Moskva 109017, Russia. (e-mail: shematov@inasan.rssi.ru)
- J.-C. Gérard, Laboratoire de Physique Atmosphérique et Planétaire, Institut d'Astrophysique, Université de Liège, 5, Avenue de Cointe, B-4000 Liège, Belgium. (e-mail: gerard@astro.ulg.ac.be)

(Received July 15, 1994; revised November 2, 1994; accepted November 30, 1994.)